Aspartate racemase, generating neuronal D-aspartate, regulates adult neurogenesis

Paul M. Kim[a,b,1], Xin Duan[a,b,1], Alex S. Huang[a], Cindy Y. Liu[b], Guo-li Ming[a,b,c], Hongjun Song[a,b,c,2] and Solomon H. Snyder[a,d,e,2]

[a]The Solomon H. Snyder Department of Neuroscience, [b]Institute for Cell Engineering, [c]Department of Neurology, [d]Department of Pharmacology and Molecular Sciences and [e]Department of Psychiatry and Behavioral Sciences, The Johns Hopkins University School of Medicine, Baltimore, MD 21205

D-Aspartic acid is abundant in the developing brain. We have identified and cloned mammalian aspartate racemase (DR), which converts L-aspartate to D-aspartate and colocalizes with D-aspartate in the brain and neuroendocrine tissues. Depletion of DR by retrovirus-mediated expression of short-hairpin RNA in newborn neurons of the adult hippocampus elicits profound defects in the dendritic development and survival of newborn neurons and survival. Because D-aspartate is a potential endogenous ligand for NMDA receptors, the loss of which elicits a phenotype resembling DR depletion, D-aspartate may function as a modulator of adult neurogenesis.

neuronal development | neural progenitor cells | hippocampus | NMDA receptor | neuroendocrine

D-amino acids are being increasingly recognized as putative neurotransmitters. D-serine, an endogenous ligand for the glutamate-NMDA receptor, is formed by serine racemase, a pyridoxal 5′-phosphate (PLP)-dependent enzyme that converts L-serine to D-serine (1). Deletion of serine racemase alters NMDA receptor neurotransmission and long-term potentiation (2–4), and its disturbance has been implicated in schizophrenia (5–7). D-aspartate is present in selected neuronal populations in the brain as well as in neuroendocrine tissues, such as the catecholaminergic cells of the adrenal medulla, the anterior/posterior lobes of the pituitary gland, the pineal gland, and the testes (8–10). In early neonatal stages, high D-aspartate densities in the cortical plate, subventricular zone, and discrete portions of the hippocampal formation imply a developmental role (11). In adult hippocampus, D-aspartate persists in dentate gyrus, where new neurons are generated throughout life (12, 13). These newborn neurons are integrated into existing neural circuitry and are involved in learning and memory formation (12, 13). Insight into specific neural functions for D-aspartate has been hampered by ignorance of its biosynthesis. In the present study, we identify and clone mammalian aspartate racemase (DR), which converts L-aspartate to D-aspartate. Deletion of DR leads to pronounced defects in adult hippocampal neurogenesis, implicating D-aspartate as a major regulator of neuronal development.

Results and Discussion

Cloning and Characterization of DR. In a genomic sequence analysis, we were unable to find candidate mammalian DR genes based on homology to serine racemase or bacterial aspartate racemases, which are either PLP-independent or PLP-dependent enzymes (14, 15). Vacca and coworkers (16–18) demonstrated that glutamate-oxalacetate transaminase (GOT) can generate small amounts of D-aspartate in the process of transaminating L-aspartate to L-glutamate, and that formation of D-aspartate is augmented in GOT mutants, wherein histidine replaces tryptophan-140 and lysine replaces arginine-292. Tryptophan-140 normally prevents access of a proton donor, such as a water molecule, which can effectuate racemization (Fig. 1A); however, replacement of tryptophan-140 by histidine allows direct protonation by histidine for racemization. In addition, transformation of arginine-292 to lysine in GOT mutants facilitates access of water molecules by possibly interfering with substrate induced closure of the enzyme's active site and enhances racemization (18).

In a NCBI protein database search, we discovered a putative DR, a GOT-like protein in which GOT's tryptophan-140 is replaced by lysine and arginine-292 is substituted with a glutamine, suggesting possibe racemase activity (Fig. S1). Similar to the previously mentioned tryptophan-140–to-histidine mutational analysis of GOT, lysine has a proton that can be directly donated for racemization (Fig. 1A). Phylogenetically, the putative DR is more closely related to cytosolic GOT (GOT1) and mitochondrial GOT (GOT2) than to serine racemase or serine dehydratase (Fig. 1B).

Cloned and expressed putative DR, a 45.5-kDa protein, generates substantial D-aspartate and only one-fifth as much L-glutamate, with very little D-glutamate (Fig. 1C). Like serine racemase, DR is PLP-dependent. PLP binds to lysine-249, and DR is inhibited by amino-oxyacetic acid, an inhibitor of PLP-dependent enzymes (Fig. 1D). The K_m of recombinant DR for L-aspartate is 3.1 mM, V_{max} is 0.46 mmol/mg/min, the optimum pH is 7.5, and the optimum temperature is 37°C (Fig. S2). The importance of lysine-136, the presumed proton donor, is highlighted by its mutation to tryptophan, which virtually abolishes racemase activity (Fig. 1E). DR is expressed most abundantly in brain, heart, and testes, with somewhat lower levels in the adrenal glands and negligible expression in liver, lung, and kidney (Fig. 1F).

Localization of DR. If DR physiologically forms D-aspartate, then the enzyme and its product should have similar localizations. D-aspartate is highly concentrated in the supraoptic and paraventricular hypothalamic nuclei, whose axons terminate in the posterior pituitary (19). Our immunohistochemical studies revealed similarly high densities of DR in the paraventricular and supraoptic nuclei (Fig. 2). D-aspartate and DR are similarly localized in pyramidal and stellate cells in the cerebral cortex as well as in hippocampal neurons in CA3/2 and the hilus of the dentate gyrus. In adult hippocampus, DR is expressed in the dentate gyrus and CA1, but D-aspartate levels in these areas are not as high as in younger mice (11). Both D-aspartate and DR are concentrated in pinealocytes of the pineal gland, in pituicytes of the posterior pituitary gland (20), and in epinephrine-producing chromaffin cells of the medulla of the adrenal glands (Fig. S3). DR and D-aspartate also are highly expressed in elongate spermatids of the testes (10, 21).
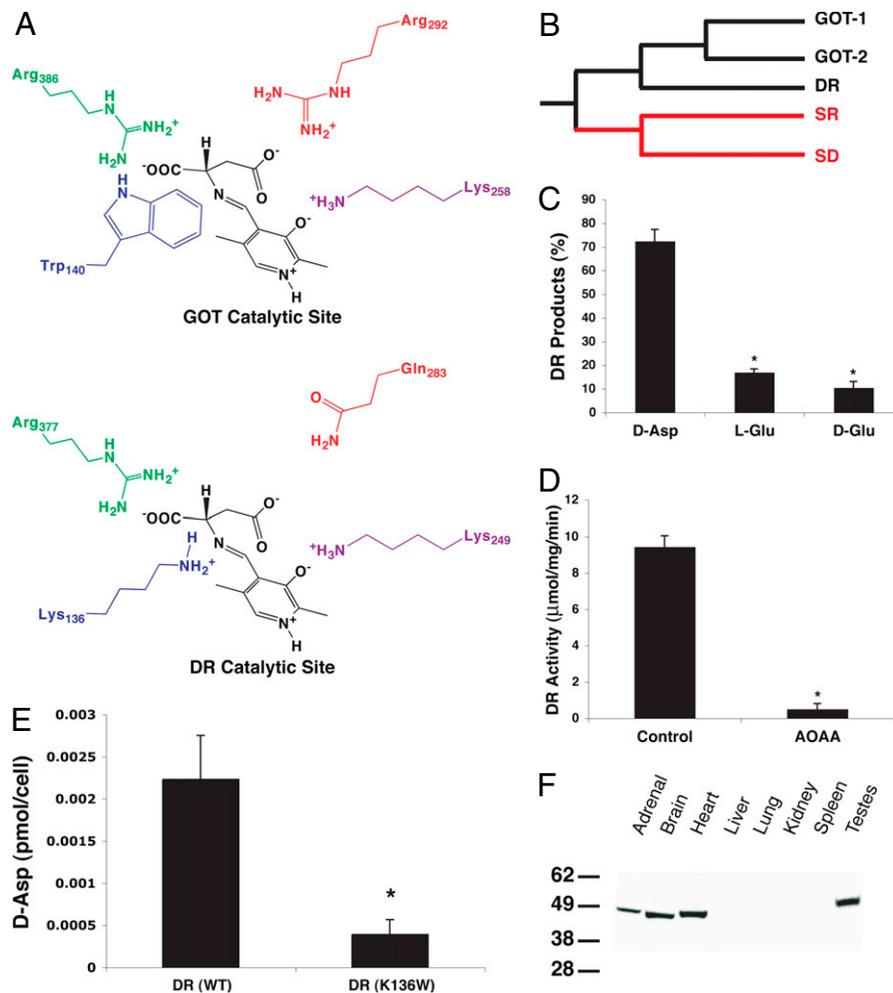
NEUROSCIENCE

Fig. 1. Cloning and characterization of DR. (*A*) Catalytic sites of GOT and DR. Trp_{140} of GOT hinders D-aspartate formation by preventing protonation at the *re* face of the α-carbon, whereas Lys_{136} of DR can provide protons for D-aspartate synthesis. (*B*) Phylogenetic analysis shows that DR is more closely related to GOT 1 and 2 than to serine racemase (SR) or serine dehydratase (SD). (*C*) DR forms much more D-aspartate than L- and D-glutamate. Values represent mean $\pm$ SEM. *$P < .005$; $n = 6$. (*D*) Amino-oxyacetic acid, an inhibitor of pyridoxal 5′-phosphate, prevents D-aspartate synthesis. Values represent mean $\pm$ SEM. *, $P < .005$; $n = 4$. (*E*) DR(WT) stable PC12 cell lines form five times more D-aspartate than DR(K136W) cells in which the proton-donating lysine is mutated to tryptophan. Values represent mean $\pm$ SEM. *, $P < .05$; $n = 4$. (*F*) Multitissue Western blot analysis shows high expression of DR in brain, heart, and testes, with moderate levels in adrenal glands.

**Dendritic Development of DR-Depleted Hippocampal Newborn Neurons.** Besides its prominence in the developing nervous system, D-aspartate is also expressed in the adult dentate gyrus. This led us to seek a role for DR in adult hippocampal neurogenesis using a retrovirus based "single-cell" genetic approach for specific manipulation of proliferating adult neural progenitor cells (22, 23). We engineered several retroviruses to deplete DR, mediated by short-hairpin RNA (shRNA) specifically against endogenous mouse DR (Fig. S4). Using several constructs, we found that specific shRNAs can knock down both overexpressed DR protein in HEK293 cells (Fig. S4*A*) and endogenous DR in cultured adult mouse hippocampal neural progenitors (24, 25) (Fig. S4*B*) and pheochromocytoma cell-12 (PC12) cells, which also results in decreased D-aspartate levels (Fig. S4*C*). These shRNAs specifically knock down DR levels and do not affect other proteins, as demonstrated by the similar levels of GAPDH and β-tubulin in DR shRNA–treated cells.

We examined the dendritic development of newborn neurons in adult mouse brain using the most effective of the shRNA constructs, shRNA-DR(5) (Fig. 3*A*). At 2 weeks after stereotaxic infection of engineered retroviruses that coexpress GFP and shRNA into the dentate gyrus of the adult mouse hippocampus, the DR-depleted GFP$^+$ newborn neurons expressing shRNA-DR (5) displayed greatly reduced dendritic arborization compared

with GFP$^+$ newborn neurons expressing control shRNA (shRNA-control). Quantitative analysis revealed significant decreases in total dendritic length (Fig. 3*B*) and branch numbers (Fig. 3*C*).

We wondered whether the reduced dendritic arborization of newborn neurons reflects a fundamental growth defect or a less-severe developmental delay. To explore these alternatives, we monitored the time course of dendritic development of GFP$^+$ neurons following retroviral injection (Fig. 3*D*). In the GFP$^+$ newborn neurons expressing shRNA-control, total dendritic length increased progressively, with an eight-fold increase between the first and fourth weeks postinjection (wpi). In contrast, the total dendritic length of shRNA-DR(5)–expressing newborn neurons was stunted between 1 and 4 wpi. At 4 wpi, total dendritic length in the DR-depleted newborn neurons was only about 40% that of controls.

To ensure that the effects of DR depletion do not represent "off-target" actions of the shRNA constructs, we examined the influence of three different constructs raised against distinct regions of DR on DR protein level (Fig. S4*B*), total dendritic lengths, and total branch numbers of newborn neurons in the adult hippocampus (Fig. S4*E*). We found similar defects with all three shRNAs.
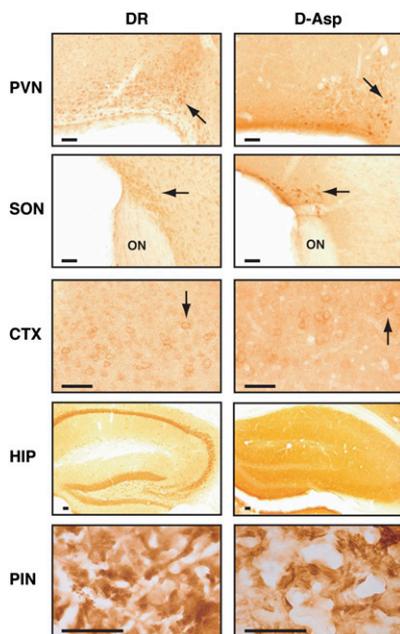
Fig. 2. DR localization. DR and D-aspartate are colocalized immunohistochemically in the brain. DR and D-aspartate are expressed in both paraventricular nuclei (PVN) and supraoptic nuclei (SON), whose axon fibers terminate in the posterior pituitary. The arrows point to neurons of PVN and SON. The linear staining of D-aspartate at the ventricular border is evidently an edge artifact. PVN is adjacent to the third ventricle, and SON is positioned above the optic nerve (ON). In the cerebral cortex (CTX), DR and D-aspartate are concentrated in pyramidal cells (arrow). DR and D-aspartate are densely localized in CA3/2 neurons of the hippocampus (HIP). In the pineal gland (PIN), both DR and D-aspartate are highly expressed in pinealocytes. (Scale bar: 50 μm.)

Survival of DR-Depleted Hippocampal Newborn Neurons. During the dendritic development studies, we noticed impaired survival in DR-depleted newborn neurons. To explore this quantitatively, we used a technique in which a mixture of engineered retroviruses coexpressing RFP and shRNA-control and retroviruses coexpressing GFP and shRNA-DR(5) is coinjected into the dentate gyrus of the adult mouse hippocampus to compare the survival of newborn neurons with and without DR depletion (Fig. 4) (26). We evaluated animals for 1–4 wpi, a period during which a significant percentage of newborn neurons experience cell death. Direct comparison of control newborn neurons expressing shRNA-control (red) and DR-depleted neurons expressing shRNA-DR(5) (green) shows that markedly increased cell death in DR-depleted neurons, whose survival was decreased by more than 50% at 2, 3, and 4 wpi (Fig. 4 *B* and *C*).

In summary, we have cloned and characterized DR, which appears to be the physiological source of mammalian D-aspartate based on its selective formation of D-aspartate and the coincident neuronal localizations of DR and D-aspartate in the brain and in multiple neuroendocrine organs. The striking alterations of adult neurogenesis in DR-depleted newborn neurons indicate an important role for DR in neuronal development, consistent with the high levels of D-aspartate during early neuronal ontogeny. The failure of DR-depleted neurons to develop normal dendritic arborization suggests an inability to integrate into the existing neuronal circuitry of the hippocampus, which may lead to decreased survival.

What accounts for the developmental defects in adult neurogenesis with DR depletion? The phenotypes that we have observed closely resemble defects observed by Gage et al. (26) in mice with similar virally elicited depletion of the NR1 subunit of glutamate-NMDA receptors in newborn neurons in the adult

dentate gyrus. D-aspartate is an agonist at NMDA receptors, with similar potency as glutamate and NMDA itself (27). Conceivably, D-aspartate, released by neuronal progenitors and their neuronal progeny, acts in an autocrine or paracrine fashion on NMDA receptors of the newborn neurons to regulate their development and survival. This notion would explain the similar phenotypes associated with depletion of NMDA receptors or DR. D-aspartate may be the principal agonist regulating NMDA receptors of the newborn neurons, so that defects elicited by NMDA receptor depletion would arise from a loss of the actions of D-aspartate generated by the neural progenitors and their neuronal progenies. Although total D-aspartate is less abundant than total glutamate, locally generated D-aspartate may be highly concentrated in the vicinity of the NMDA receptors of newborn neurons. This model affords a relatively precise mode of signaling that is less sensitive to random environmental perturbations known to elicit potentially neurotoxic leakage of glutamate from multiple cellular compartments (28). Presumably, the formation/release of D-aspartate is determined by regulation of DR. Insight into posttranslational modifications of DR and its regulation by protein–protein interactions may shed further light on the process of adult neurogenesis.

Materials and Methods

Cloning of DR. DR was cloned in silico by searching the National Center for Biotechnology Information protein database (www.ncbi.nlm.nih.gov) for proteins homologous to GOT and containing racemase-specific amino acid residues. DR gene was cloned by PCR from IMAGE clones 6447804 and 6445179. Multisequence alignment was conducted using ClustalW alignment (MacVector). Phylogenetic analysis was done using a neighbor-joining method (www.biophys.kyoto-u.ac.jp).

DR Purification. DR was cloned into pET vector (Novagen), which was transformed into BL21 *Escherichia coli*. A 50-mL starter culture was grown overnight at 37 °C. The next day, the culture was placed in 1 L of LB medium, and bacteria were grown for 2 h at 37 °C. After induction with 1 mM isopropylthio-β-galactoside (Invitrogen) for 3 h at 37 °C, the cells were centrifuged at $1,000 \times g$ for 10 min and then lysed using BugBuster (Novagen). His-tagged DR was bound to Talon metal affinity resin (BD Biosciences), and the recombinant protein was eluted with 250 mM imidazole. Purification was verified by SDS/PAGE gel.

DR Assay. DR racemase activity was assayed in 0.5 μL of PLP (100 nM), 490 μL of recombinant DR (0.5 mg/mL), and 10 μL of L-aspartate (1 mM) at 37°C for 1 h in 500 μL of 10 mM Tris (pH 7.5). In enzyme kinetic experiments, L-aspartate concentrations varied from 10 mM to 0.01 mM. In glutamate formation experiments, 1 mM α-ketoglutarate was added with 1 mM L-aspartate. Enzyme inhibition experiments used 1 mM amino-oxyacetic acid (Sigma-Aldrich). The enzymatic reactions were stopped by adding 10% trichloroacetic acid, and the acid was subsequently removed by three rounds of ether extraction. Samples were dried and resuspended in 0.4 M boric acid (pH 9.0). D-aspartate formation was analyzed by reverse-phase C_{18} HPLC (Waters) as described previously (29).

DR Stable PC12 Cell Line. DR was cloned into pcDNA vector (Invitrogen). The vector was linearized and transfected into PC12 cells using Lipofectamine 2000 (Invitrogen). Cells containing DR were selected using G418 (0.5 mg/mL; Clontech).

DR Antibody Production. His-tagged recombinant DR was used to produce a polyclonal antibody in rabbits (Cocalico Biologicals). The antibody was initially purified using an Econo-Pac Serum IgG purification column (Bio-Rad), followed by a His-DR column.

Immunohistochemistry of DR and D-Aspartate. All animal procedures were performed in accordance with institutional guidelines. C57BL/6 mice were perfused with 5% glutaraldehyde/0.5% paraformaldehyde for 30 min at 37°C. Organs were postfixed for 2 h and cryoprotected with 30% sucrose in PBS. The free-floating sections were quenched with 0.1% H_2O_2 in methanol/PBS, blocked with 4% normal goat serum and 0.2% Triton X-100 in TBS (blocking buffer), and incubated with DR antibody, diluted 1:700 in blocking buffer, overnight at 4 °C. For immunohistochemistry, DR antibody works optimally

NEUROSCIENCE

Fig. 3. DR regulates dendritic development of newborn neurons in the adult hippocampus. (*A*) Representative samples of confocal projection images of newborn neurons infected with retroviruses coexpressing GFP and either shRNA-control or shRNA-DR(5) at 2 wpi. (*B* and *C*) Newborn neurons infected with shRNA-DR(5) exhibit significantly decreased total dendritic length and number of branches at 2 wpi. (*D*) The time course of dendritic development of newborn neurons expressing shRNA-control and shRNA-DR(5). Note the significant dendritic growth in control newborn neurons from 1 wpi to 4 wpi compared with dendrites of DR-depleted neurons. Values represent mean ± SEM. *, $P < .05$; $n = 4$ mice for each time point, ANOVA.

at 1:700 dilution. The specificity of the antibody is demonstrated by tissue Western blot analysis, where DR antibody recognized only one band at a size corresponding to molecular weight of DR. Labeling was visualized with the Vectastain Elite kit (Vector Laboratories).

D-Aspartate immunohistochemistry was conducted as described previously (19). C57BL/6 mice were perfused with 5% glutaraldehyde/0.5% paraformaldehyde at 37 °C. Organs were postfixed for 2 h and cryoprotected. Free-floating sections (45 μm) were quenched with 0.1% H_2O_2 in methanol/PBS, reduced with 0.5% $NaBH_4$, blocked with blocking buffer, and incubated with a D-asp antibody (1:750 dilution) overnight at 4 °C in the presence of L-aspartate–glutaraldehyde conjugate (200 μM). Labeling was visualized with the Vectastain Elite kit. Specificity was determined by abolishing the signal with D-aspartate–glutaraldehyde conjugate (200 μM).

Construction, Characterization, and Production of DR shRNA and Control Oncoretroviruses. Self-inactivating murine-engineered oncoretroviruses were used to express DR shRNA and GFP or control shRNA and mCherry specifically in proliferating cells and their progeny (22–25). GFP (pUEG) or mCherry (pUEM) expression was under the control of EF1 promoter, and a specific shRNA was coexpressed under the control of human U6 promoter in the same vector. Several shRNAs against different regions of DR (Fig. S4A) and a control shRNA against DsRed were used (22, 23). The following short-hairpin sequences were cloned into retroviral vectors (22): shRNA-C1, AGTTCCAG-TACGGCTCCAA (shDsRed); shRNA-DR(A), GAAGGCAGCTTACTAAAGA; shRNA-DR(B), CTAGAAGGCAGCTTACTAA; and shRNA-DR(5), TGTATCGTCTC-ATGTCAAA.

Specificity and efficiency of DR shRNAs were determined by coexpressing DR shRNA vectors and HA-tagged DR in HEK 293 cells and checking for DR expression (Fig. S4A). DR shRNA vectors also were transfected in PC12 cells, which express endogenous DR, and levels of DR and D-aspartate were determined by Western blot analysis and HPLC, respectively (Fig. S4C).

High titers of engineered oncoretroviruses (1×10^9 units/mL) were produced by cotransfection of retroviral vectors and vesicular stomatitis viral envelope into 293GP cells, as described previously (23). Specificity and efficiency of these oncoretroviruses were determined by infecting cultured adult neural progenitors, as described previously (24, 25), and monitoring endogenous DR expression (Fig. S4B).

Stereotaxic Injection of Engineered Oncoretroviruses. Adult female C57BL6 mice (7–8 weeks old; Charles River) housed under standard conditions were anesthetized (100 mg ketamine, 10 mg xylazine in 10 mL saline/g). Then

Fig. 4. DR regulates survival of newborn neurons in the adult hippocampus. (*A*) Sample confocal images of newborn neurons coexpressing RFP and shRNA-control (red) and newborn neurons coexpressing GFP and shRNA-DR(5) (green) in the same animal. Coinfected neurons express both RFP and GFP (yellow). (*B* and *C*) Newborn neurons expressing shRNA-DR have markedly decreased survival. Values represent mean ± SEM. *, $P < .05$; $n = 4$ mice for each time point, ANOVA. More than half of the DR shRNA–infected newborn neurons die by 2 wpi. Note the two different approaches to directly comparing the survival of normal and DR-depleted newborn neurons in the same animal. The same mixture of retroviruses was injected in a cohort of animals and examined at 1, 2, 3, and 4 wpi. The ratio of DR-depleted neurons and control neurons in the same animal at 1 wpi was normalized to 100% for comparison at later time points.

engineered retroviruses or a mixture of two different retroviruses were stereotaxically injected into the dentate gyrus at four sites (0.5 μL per site at 0.25 μL/min), with the following coordinates (posterior, 2 mm from Bregma; lateral, ±1.6 mm; ventral, 2.5 mm; posterior, 3 mm from Bregma; lateral, ± 2.6 mm; ventral, 3.2 mm), as described previously (23).

Immunostaining, Confocal Imaging, and Analysis. Coronal brain sections (40 μm thick) were prepared from viral injected mice and processed for immunostaining as described previously (23). The sections were incubated for 30 min in DAPI (1:5,000 dilution) before washing and mounting. Images were acquired on a META multiphoton confocal system (Zeiss LSM 510) using a multitrack configuration.

For analysis of dendritic development in vivo, three-dimensional reconstruction of the entire dendritic processes of each neuron was made from Z-series stacks of confocal images. The projection images were semiautomatically traced with ImageJ using the NeuronJ Plugin (http://imagescience.bigr.nl/meijering/software/neuronj/). All GFP⁺ dentate granule cells with largely intact dendritic trees were analyzed for total dendritic length and branch number as described previously (22). The measurements did not include corrections for inclinations of dendritic process and thus represented projected lengths. Data shown represent individual GFP⁺ den-

tate granule cells from at least four animals for each experimental group. Statistic significance was determined by ANOVA.

Survival Analysis of New Neurons. Sections were selected evenly from anterior to posterior regions of the dentate gyrus. The numbers of RFP (mCherry)-positive (control) only, GFP [DR shRNA(5)] only, and double-positive new neurons in the granule cell layer and the subgranular zone were counted for each section (25). The densities of new neurons (mCherry-positive only, GFP-positive only, and double-positive) were affected by the precise titer of viruses. The absolute numbers of fluorescently labeled neurons generally were highly variable when different viral preparations were injected, even if we tried to measure and match virus titer precisely; however, with the same viral preparation, the densities of fluorescently labeled new neurons were reliable between mice. Therefore, we used the same viral preparations for each experiment.

1. Wolosker H, Blackshaw S, Snyder SH (1999) Serine racemase: A glial enzyme synthesizing D-serine to regulate glutamate-N-methyl-D-aspartate neurotransmission. *Proc Natl Acad Sci USA* 96:13409–13414.
2. Panatier A, et al. (2006) Glia-derived D-serine controls NMDA receptor activity and synaptic memory. *Cell* 125:775–784.
3. Inoue R, Hashimoto K, Harai T, Mori H (2008) NMDA- and beta-amyloid1-42–induced neurotoxicity is attenuated in serine racemase knock-out mice. *J Neurosci* 28:14486–14491.
4. Yang Y, et al. (2003) Contribution of astrocytes to hippocampal long-term potentiation through release of D-serine. *Proc Natl Acad Sci USA* 100:15194–15199.
5. Labrie V, et al. (2009) Serine racemase is associated with schizophrenia susceptibility in humans and in a mouse model. *Hum Mol Genet* 18:3227–3243.
6. Fujii K, et al. (2006) Serine racemase binds to PICK1: Potential relevance to schizophrenia. *Mol Psychiatry* 11:150–157.
7. Tsai G, Yang P, Chung LC, Lange N, Coyle JT (1998) D-serine added to antipsychotics for the treatment of schizophrenia. *Biol Psychiatry* 44:1081–1089.
8. Dunlop DS, Neidle A, McHale D, Dunlop DM, Lajtha A (1986) The presence of free D-aspartic acid in rodents and man. *Biochem Biophys Res Commun* 141:27–32.
9. Hashimoto A, et al. (1993) Free D-serine, D-aspartate and D-alanine in central nervous system and serum in mutant mice lacking D-amino acid oxidase. *Neurosci Lett* 152:33–36.
10. D'Aniello A, et al. (1996) Involvement of D-aspartic acid in the synthesis of testosterone in rat testes. *Life Sci* 59:97–104.
11. Wolosker H, D'Aniello A, Snyder SH (2000) D-aspartate disposition in neuronal and endocrine tissues: Ontogeny, biosynthesis and release. *Neuroscience* 100:183–189.
12. Ming GL, Song H (2005) Adult neurogenesis in the mammalian central nervous system. *Annu Rev Neurosci* 28:223–250.
13. Zhao C, Deng W, Gage FH (2008) Mechanisms and functional implications of adult neurogenesis. *Cell* 132:645–660.
14. Long Z, et al. (2001) Occurrence of D-amino acids and a pyridoxal 5′-phosphate–dependent aspartate racemase in the acidothermophilic archaeon, *Thermoplasma acidophilum. Biochem Biophys Res Commun* 281:317–321.
15. Yamauchi T, et al. (1992) Properties of aspartate racemase, a pyridoxal 5′-phosphate–independent amino acid racemase. *J Biol Chem* 267:18361–18364.
16. Kochhar S, Christen P (1992) Mechanism of racemization of amino acids by aspartate aminotransferase. *Eur J Biochem* 203:563–569.
17. Vacca RA, Christen P, Malashkevich VN, Jansonius JN, Sandmeier E (1995) Substitution of apolar residues in the active site of aspartate aminotransferase by histidine: Effects on reaction and substrate specificity. *Eur J Biochem* 227:481–487.
18. Vacca RA, et al. (1997) Active-site Arg →Lys substitutions alter reaction and substrate specificity of aspartate aminotransferase. *J Biol Chem* 272:21932–21937.
19. Schell MJ, Cooper OB, Snyder SH (1997) D-aspartate localizations imply neuronal and neuroendocrine roles. *Proc Natl Acad Sci USA* 94:2013–2018.
20. Lee JA, Homma H, Tashiro K, Iwatsubo T, Imai K (1999) D-aspartate localization in the rat pituitary gland and retina. *Brain Res* 838:193–199.
21. Sakai K, et al. (1998) Localization of D-aspartic acid in elongate spermatids in rat testis. *Arch Biochem Biophys* 351:96–105.
22. Ge SY, et al. (2006) GABA regulates synaptic integration of newly generated neurons in the adult brain. *Nature* 439:589–593.
23. Duan X, et al. (2007) *Disrupted-In-Schizophrenia 1* regulates integration of newly generated neurons in the adult brain. *Cell* 130:1146–1158.
24. Ma DK, Chiang CH, Ponnusamy K, Ming GL, Song H (2008) G9a and Jhdm2a regulate embryonic stem cell fusion-induced reprogramming of adult neural stem cells. *Stem Cells* 26:2131–2141.
25. Kim JY, et al. (2009) DISC1 regulates new neuron development in the adult brain via modulation of AKT-mTOR signaling through KIAA1212. *Neuron* 63:761–773.
26. Tashiro A, Sandler VM, Toni N, Zhao C, Gage FH (2006) NMDA-receptor-mediated, cell-specific integration of new neurons in adult dentate gyrus. *Nature* 442:929–933.
27. Erreger K, et al. (2007) Subunit-specific agonist activity at NR2A-, NR2B-, NR2C-, and NR2D-containing N-methyl-D-aspartate glutamate receptors. *Mol Pharmacol* 72:907–920.
28. Danysz W, Parsons CG (1998) Glycine and N-methyl-D-aspartate receptors: physiological significance and possible therapeutic applications. *Pharmacol Rev* 50:597–664.
29. Hashimoto A, Nishikawa T, Oka T, Takahashi K, Hayashi T (1992) Determination of free amino acid enantiomers in rat brain and serum by high-performance liquid chromatography after derivatization with N-tert.-butyloxycarbonyl-L-cysteine and o-phthaldialdehyde. *J Chromatogr* 582:41–48.

NEUROSCIENCE